# Spin fluctuation nearby magnetically unstable point in $Li_{1-x}Zn_xV_2O_4$

N. Fujiwara, H. Yasuoka, and Y. Ueda
*Institute for Solid State Physics, University of Tokyo, Roppongi, Minato-ku, Tokyo 106, Japan*
(Received 9 September 1998)

Nuclear magnetic resonance (NMR) for $^7$Li nuclei was performed in vanadium spinel $Li_{1-x}Zn_xV_2O_4$ ($0 \leqslant x \leqslant 0.4$) from 4.2 to 300 K. The relaxation rate ($1/T_1$) and the linewidth for a paramagnetic metal $LiV_2O_4$ take the maximum at 50 and 20 K, respectively, whereas those for $x \neq 0$ samples show monotonous increase with decreasing temperature toward a spin glass order which appears at about 15 K. These qualitative differences with respect to Zn concentration were investigated in relation to a metal nearby the ferromagnetically unstable point. [S0163-1829(99)05109-7]

## I. INTRODUCTION

Vanadium spinel $Li_{1-x}Zn_xV_2O_4$ has been one of the attractive materials for the study of metal insulator transition (MIT) since the end materials $ZnV_2O_4$ and $LiV_2O_4$ are believed to be an insulator with antiferromagnetic order at low temperature ($\sim$40 K) and a paramagnetic metal with no magnetic orders, respectively, and the substitution of Zn for Li does not accompany any crystal phase transitions except for $x > 0.9$.[1–6] Single crystals of $LiV_2O_4$ were synthesized by Roger *et al.* in 1964 using a hydrothermal technique and they reported metal-like conductivity.[1] Ever since, this material has been regarded as a metal. The order of the resistivity they measured is about $10^{-5}$–$10^{-6}\rho$m, whereas that for the powder samples[2] is one order larger than the single crystals. Recently, the metal-like conductivity has been reproduced by using single crystals which were synthesized by a hydrothermal technique.[7] It has been reported from the Seebeck coefficient[2,3] and far infrared absorption[3] that the MIT occurs in this system without any crystal transitions at $x = 0.4$–$0.5$. The value is deeply related with magnetic properties since the susceptibility at fixed temperatures above 100 K takes a maximum at $x \sim 0.4$. As for the $T$ dependence of the susceptibility, no qualitative change occurs at $x \sim 0.4$. The temperature ($T$) dependence of the susceptibility for $0.2 \leqslant x \leqslant 0.9$ shows the upturn toward a spin glass order which appears at low temperatures below 15 K.

Although $Li_{1-x}Zn_xV_2O_4$ is very interesting from the viewpoint of the MIT, one of the end materials, $LiV_2O_4$ has been recently recognized as an anomalous material from the specific heat $C(T)$ (Ref. 8) and nuclear spin-lattice relaxation rate $1/T_1$ of $^7$Li.[8–11] A large value of the specific heat coefficient $\gamma(0)$ ($\equiv [C(T)/T]|_{T=0} \sim 420$ mJ/mol K$^2$) and nonlinear $T$ dependence of $C/T$ have been reported from the specific heat measurement. The value of $\gamma(0)$ is the largest in $d$-electron systems and is comparable with those of $UPt_3$ and $CeCu_2Si_2$.[12] Then, this material is regarded as a $d$-electron heavy fermion system. The anomalous behavior of $1/T_1$ for $^7$Li has been nearly simultaneously reported by several groups and almost the same results have been obtained. $1/T_1$ shows almost $T$ linear dependence at low temperatures below 50 K and takes a maximum at 50 K and then approaches to a finite value at about 700 K.[10,11] Furthermore, the susceptibility shows Curie-Weiss-like behavior, although the system shows metal-like conductivity.[1,7] The effective moment $p_{\rm eff}$ is 1.5 and the Weiss constant is about $-30$ K, if the localized model is applied. The interpretation for the Curie-Weiss-like behavior depends on the models.

A model analogous to $f$-electron heavy fermion compounds has been presented.[8] The Curie-Weiss-like behavior, the large $\gamma(0)$, and the anomalous behavior of $1/T_1$ have been investigated in relation to the Kondo effect.[8,13] The anomalous behavior of $1/T_1$ has been interpreted by considering two mechanisms; one is the relaxation mechanism due to the conduction electrons and the other is the relaxation mechanism due to the localized $d$ electrons which fluctuate by the spin-spin exchange interaction and elastic scattering with conduction electrons.[11] The application of the Kondo model to this system requires the existence of two kinds of $d$ electrons with localized and conductive characters in the $t_{2g}$ state. The double exchange mechanism has also been applied to this system[2,5] and the model also implicitly requires two types of $d$ electrons with localized and conductive characters.

Another model is a treatment as a metal in a paramagnetic state nearby the ferromagnetically unstable point.[10] The existence of the localized $d$ electron in the real space is not necessary in this model. Although the ferromagnetic order is not realized, the system has been treated as a metal nearby the unstable point because the experimental results exhibit similarities to well known ferromagnetic metals; the susceptibility obeys the Curie-Weiss-like behavior and $1/T_1$ is almost constant at high temperatures. In ferromagnetic metals the Curie-Weiss behavior originates from the $T$ linear dependence of the mean-square local amplitude of spin fluctuation $S_L^2 = \Sigma_q \langle S_q^2 \rangle / N = 3\ k_B T \Sigma_q \chi_q / N$. The values of the effective Bohr magnetons $p_{\rm eff}$ in weakly ferromagnetic metals such as MnSi,[14] $ZrZn_2$,[15] and $Sc_3In$ (Ref. 16) or a nearly ferromagnet $TiBe_2$ (Ref. 17) are 2.1, 1.4, 0.7, and 1.88, respectively. The order of the susceptibility and the value of $p_{\rm eff}$ in $LiV_2O_4$ are rather close to weakly ferromagnetic metals such as MnSi, $ZrZn_2$, and $Sc_3In$ or a nearly ferromagnetic metal $TiBe_2$. From the viewpoint of this model, the Curie-Weiss behavior for $LiV_2O_4$ originates from the local amplitude of the spin fluctuation $S_L$ with a dominant contribution from the uniform mode $q = 0$, and the origin which brings the anomaly to $\gamma(0)$ and $1/T_1$ is the critical location nearby the ordered

 

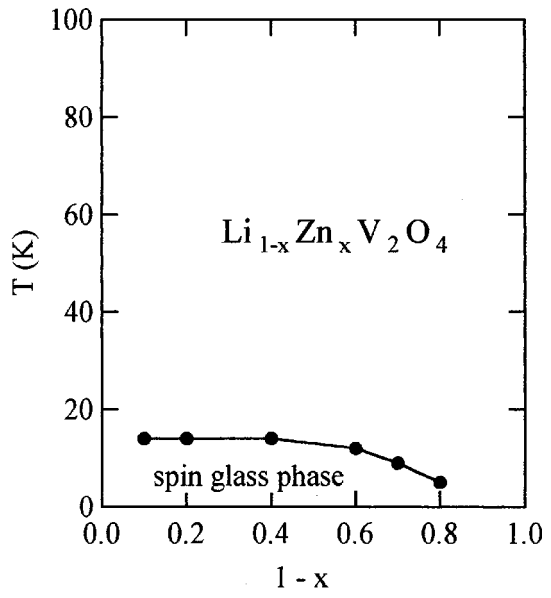


FIG. 1. Phase diagram of $Li_{1-x}Zn_xV_2O_4$ extracted from Ref. 4. The solid line is a guide for the eyes.

state (the spin glass order in the present case) in the phase diagram. It should be noted that the system is not an antiferromagnetic metal since $1/T_1$ should be proportional to $\sqrt{T}$ at high temperatures and the $T$ dependence of the susceptibility should be very weak although the staggered susceptibility shows the Curie-Weiss-like behavior in this case.[18]

In the previous paper[10] we analyzed $1/T_1$ of pure $LiV_2O_4$ from the viewpoint of a metal nearby the ferromagnetically unstable point on the basis of the self-consistent renormalization (SCR) theory presented by Ishigaki and Moriya.[19] The $T$ dependence of $1/T_1$ in a wide range from 4 up to 700 K has been analyzed on the basis of the theory and the values of two parameters $y_0$ and $T_0$, which are parameters required in the SCR theory, have been estimated as $6\times10^{-5}$ and 800 K, respectively. (The meanings of them are mentioned in Sec. III.) Two parameters are related to the specific heat coefficient $\gamma(0)$ per mole as[20]

$$\gamma(0)=-\frac{3Nk_B}{4T_o}\ln y_0. \tag{1}$$

The value was obtained as 150 mJ/mol $K^2$ by applying the above-mentioned values for $y_0$ and $T_0$. The value is the same order with the experimental results.

In the present work we have performed NMR measurements on $Li_{1-x}Zn_xV_2O_4$ in the lightly doped region $0\leqslant x\leqslant0.4$, where the system is believed to be metal-like. We also investigated whether the system is explained systematically in the viewpoint of a metal nearby the ferromagnetically unstable point.

## II. EXPERIMENTAL RESULTS

The phase diagram of $Li_{1-x}Zn_xV_2O_4$ is shown in Fig. 1. The data were extracted from Ref. 4. The lattice parameter changes from 0.825 to 0.840 nm at room temperature as Zn concentration increases from $x=0$ to $x=1.0$. The structural transition from the cubic phase to tetragonal phase is seen for

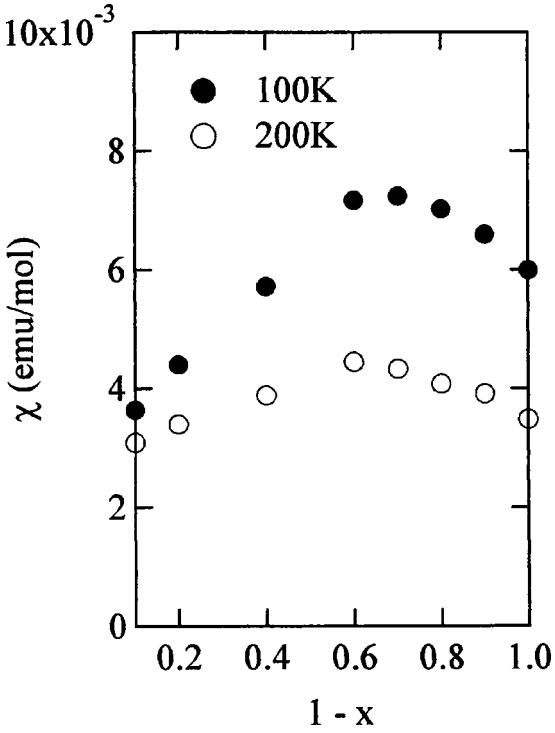


FIG. 2. The susceptibility measured at fixed temperatures above 100 K.

$x\geqslant0.9$. The spin glass phase appears in a wide range of $x$ ($0.2\leqslant x\leqslant0.9$) at low temperatures below 15 K. The transition temperature $T_g$ gradually increases with increasing Zn concentration for the metal-like region $0\leqslant x\leqslant0.4$ and approaches to a constant ($T_g\sim15$ K) for the nonmetallic region $x\geqslant0.4$. The transition temperature increases as $T_g\simeq20\sqrt{x-0.09}$. Although the spin glass transition has not been observed for $x=0.1$ at temperatures above 4.2 K, the susceptibility, $1/T_1$ and $^7$Li-NMR linewidth increase remarkably with decreasing temperature. The transition is expected to occur even for $x=0.1$ at a low temperature below 4.2 K.

### A. Susceptibility

The susceptibility data at fixed temperatures are shown in Fig. 2. The maximum appears at $x\sim0.4$ above 100 K. The susceptibility data for $0\leqslant x\leqslant0.4$ under zero field cool condition are shown in Fig. 3. These data were extracted from

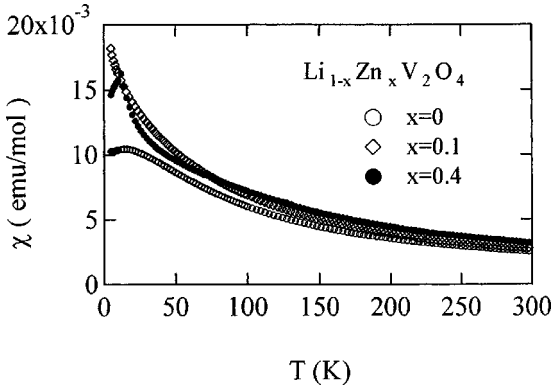


FIG. 3. Temperature dependence of the susceptibility measured under zero field cool condition.

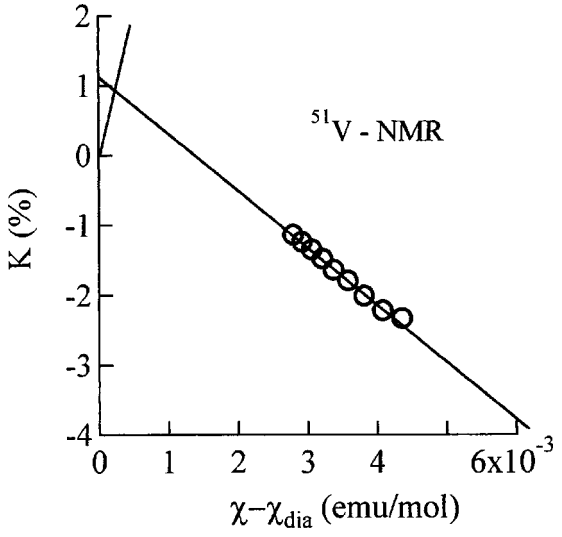


FIG. 4. $K$-$\chi$ plot of $^{51}$V for $LiV_2O_4$.

Ref. 4. The value of the susceptibility is almost the same for $x=0.2$ and 0.4 samples, although the value for $x=0.4$ is a little bit larger than that for $x=0.2$ at high temperatures above 100 K. The cusp below 15 K corresponds to the spin-glass transition. The susceptibility is decomposed as

$$\chi=\chi_{\rm orb}+\chi_d+\chi_{\rm dia}, \tag{2}$$

where the first, second, and third term are the Van Vleck orbital susceptibility, $d$-electron spin susceptibility, and the diamagnetic susceptibility, respectively. The decomposition is possible by using the results of $^{51}$V-NMR. The decomposition has been done only for pure $LiV_2O_4$ since the $^{51}$V-NMR signal has been observed only for pure $LiV_2O_4$ above 150 K. The value of $\chi_{\rm dia}$ is estimated as $-5.66\times10^{-5}$ emu/mol from the table of the diamagnetic susceptibility of $Li^+$,$V^{5+}$,$O^{2-}$ by Selwood.[21,22] The orbital shift $K_{\rm orb}$ is related with the orbital susceptibility $\chi_{\rm orb}$ as

$$K_{\rm orb}=(A_{\rm orb}/{\rm N}\mu_B)\chi_{\rm orb}=(2\mu_B/N\mu_B\langle r^3\rangle)\chi_{\rm orb}, \tag{3}$$

where $A_{\rm orb}$ and $\langle r^3\rangle$ are the orbital hyperfine coupling constant and the expectation value of $r^3$ for the $3d$ wave function, respectively. $N$ is the number of V ions per mole and is equal to $2N_A$ ($N_A$ is the Avogadro number). The above relation becomes $K_{\rm orb}=41.6\chi_{\rm orb}$ (emu/mol), if the value of the Hartree-Fock calculation for the $3d^1$ wave function is used for $\langle r^{-3}\rangle$(=3.68 a.u.). The hyperfine coupling of $^{51}$V, $A_{\rm hfV}$ is related with the spin part of the shift $K_d$ and $\chi_d$ as

$$K_d=(A_{\rm hfV}/{\rm N}\mu_B)\chi_d. \tag{4}$$

We have obtained $\chi_{\rm orb}=2.16\times10^{-4}$ emu/mol, $A_{\rm orb}=464.8$ KOe/$\mu_B$, and $K_{\rm orb}=0.90\%$, respectively, from the $K$-$\chi$ plot as shown in Fig. 4. The constant value $\chi_0$ which is obtained from the decomposition of the susceptibility ($\chi=\chi_0+\chi_{\rm Curie}$, where $\chi_{\rm Curie}$ is the Curie-Weiss term) becomes $2.3\times10^{-4}$ (emu/mol) and is almost the same as $\chi_{\rm orb}$. There remains a discrepancy of about $-7\times10^{-5}$ (emu/mol) in $\chi_{\rm orb}+\chi_{\rm dia}-\chi_0$, however, this value depends on the fitting range of $T$ where the decomposition of $\chi=\chi_0+\chi_{\rm Curie}$ is done. The hyperfine coupling constant is obtained as $A_{\rm hfV}=-89.0$KOe/$\mu_B$ from the slope of the $K$-$\chi$ plot. The values of $A_{\rm hfV}$ obtained by other groups[11,23] are almost the same as those of the present work. Similar values of $\chi_{\rm orb}$ and $\chi_d$ are expected for Zn substituted samples since a drastic change has not been observed in the susceptibility at high temperatures as shown in Fig. 3.

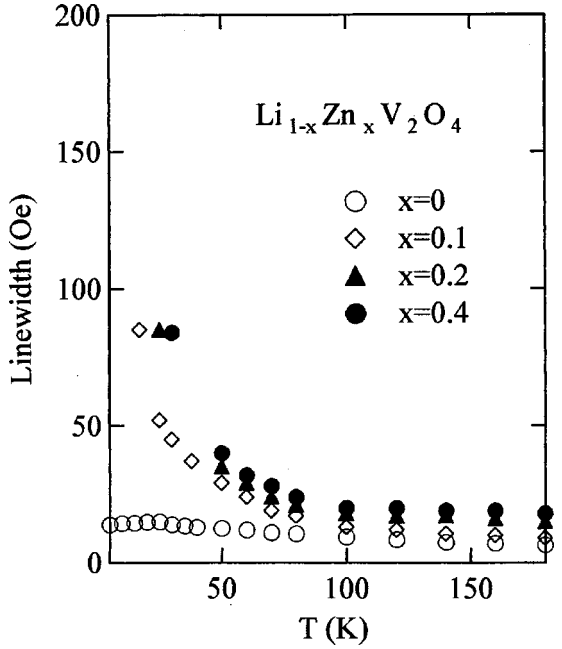


FIG. 5. Temperature dependence of the linewidth of the $^7$Li-NMR signal.

### B. NMR measurements

#### *1. Knight shift and linewidth*

The NMR measurement was curried out under zero field cool condition at the frequency 18.81 MHz. The temperature dependence of the linewidth is shown in Fig. 5. The linewidth of pure $LiV_2O_4$ is below 20 G and takes a maximum at about 20 K, while that of the Zn substituted samples shows a monotonous increase with decreasing temperature toward the transition temperature. The values of the linewidth become large with the increase in Zn concentration at fix temperatures. The $T$ dependence of the linewidth corresponds to that of the susceptibility in that these quantities exhibit an anomaly at 20 K for pure $LiV_2O_4$, whereas those for the Zn substituted samples increase with decreasing temperature toward the transition temperature. The linewidth for the pure sample has been analyzed as the sum of two contributions; one is the intrinsic linewidth $\Delta w$ which is determined by the spin echo decay $1/T_2$. The nuclear $^7$Li-$^7$Li and $^7$Li-$^{51}$V dipolar interactions which yield no $T$ and $H$ dependence are included in $\Delta w$. The other is macroscopic field inhomogeneities due to the demagnetization effects of powder samples which is proportional to the susceptibility.[24,25] The linewidth $\Delta W$ is represented by using Gaussian approximation[11]

$$\Delta{\rm W}=\sqrt{\Delta w^2+\alpha(\chi H)^2}. \tag{5}$$

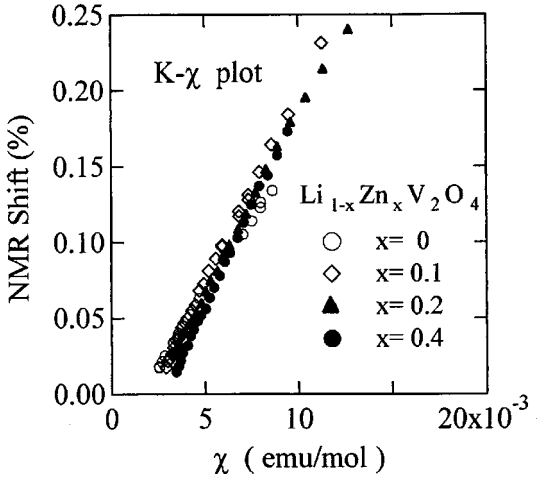


FIG. 6. $K$-$\chi$ plot of $^7$Li.

The values of $\Delta w$ and $\alpha$ are evaluated as 4.6 Oe and 0.118 $(\text{emu/mol})^{-1}$, respectively, for pure $LiV_2O_4$ at the field 11.35 KOe. This relation fits the experimental results well down to 30 K. The linewidth for the Zn doped samples, however, deviates from Eq. (5) at low temperatures below 100 K if $\Delta w$ is assumed to be a constant as is seen easily from Figs. 3 and 5. The larger broadening of the linewidth at lower temperatures is mainly attributed to a critical slowing down toward the spin glass phase.

The Knight shift for $^7$Li shows almost the same temperature dependence with the results of the susceptibility as is seen from the $K$-$\chi$ plot in Fig. 6. The shift originates from transferred hyperfine interaction and is related to the temperature-dependent part of the susceptibility $\chi_d$ as $K \propto A_{\text{tr}}\chi_d z_{\text{Li}}$ where $A_{\text{tr}}$ is the transferred hyperfine coupling constant and $z_{\text{Li}}(=12)$ is the number of the nearest neighbor V ions at a Li ion site. The value of $A_{\text{tr}}$ for pure $LiV_2O_4$ has been obtained as 0.18 KOe/$\mu_B$. The effective coupling constant $A_{\text{hf}}$ per a $^7$Li nucleus is given as $A_{\text{hf}}^2 = z_{\text{Li}}A_{\text{tr}}^2 + A_{\text{dip}}^2$, where $A_{\text{dip}}$ represents dipolar coupling. Although $A_{\text{hf}}$ for pure $LiV_2O_4$ is estimated by calculating $A_{\text{dip}}$, $A_{\text{hf}}$ is obtained experimentally from the comparison with $1/T_1$ of $^{51}$V. The relaxation rates of $^{51}$V also show similar temperature dependence with those of $^7$Li at high temperatures. The values of $1/T_1$ at 280 K are 19 $\text{sec}^{-1}$ and 24 $\text{msec}^{-1}$ for $^7$Li and $^{51}$V, respectively. The effective coupling constant of $^7$Li is estimated as 1.71 KOe/$\mu_B$ from the relation $(1/T_1)_{\text{Li}}/(1/T_1)_{\text{V}} = \gamma_{N\text{Li}}^2 A_{\text{hf}}^2/\gamma_{N\text{V}}^2 A_{\text{hfV}}^2$, where the contribution from the orbital is expected to be small and is neglected in $(1/T_1)_{\text{V}}$. A similar estimation of $A_{\text{hf}}$ for $x \neq 0$ could be possible if the $^{51}$V-NMR signal was observed. Unfortunately, the $^{51}$V signal for $x \neq 0$ has not been observed. However, $A_{\text{hf}}$ for $x \neq 0$ is expected to be almost the same as that of pure $LiV_2O_4$ since $A_{\text{tr}}$ is almost the same as shown in Fig. 6 and the calculated values of $A_{\text{dip}}$ is almost the same as the pure one.

#### *2. Relaxation rate $1/T_1$ of $^7$Li*

The relaxation time was measured by using a usual pulsed-NMR spectrometer. The results of $1/T_1$ for the Zn substituted samples are shown in Fig. 7. The recovery curve fits a single exponential function for nearly two orders of magnitude for pure $LiV_2O_4$ since $^7$Li nuclei locate on the center of tetrahedra of oxygen and are free from a electric quadrupole effect. The data for pure $LiV_2O_4$ are extracted from the previous work.[10] The recovery curves for the Zn substituted samples also fit a single exponential function for nearly two orders of magnitude, however, deviate from the single exponential function at much lower temperatures near the order point because of the remarkable increase of the linewidth. We have plotted the data whose recovery curves almost fit the single exponential function. All of $1/T_1$ for the Zn substituted samples diverge toward the transition temperatures.

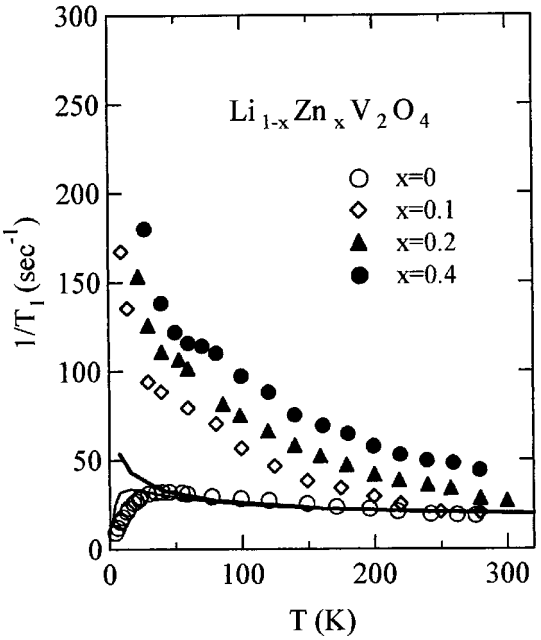


FIG. 7. Temperature dependence of $1/T_1$ for $^7$Li. Solid curves which go down to zero and go up with decreasing temperatures are calulated from Eqs. (6)–(9) by applying $y_0 = 0.00006$ and 0, respectively.

It should be noted that the susceptibility, the shift, and $1/T_1$ are deeply related to one another for the $T$ and Zn-concentration dependences in the point that these quantities for pure $LiV_2O_4$ remain finite values even at low temperatures, whereas those for the Zn substituted samples increase monotonously with decreasing temperature toward the transition temperature. The susceptibility and the shift are essentially determined by the $q=0$ component in the $q$-dependent susceptibility $\chi(q)$. On the other hand, $1/T_1$ is, in general, determined by all modes including $q=\pi$. The experimental fact that $1/T_1$ shows a similar $T$ dependence with the susceptibility and the shift implies that spin fluctuation with $q=0$ plays a significantly important role in the present system. This fact gives one of the grounds that the system is treated in a way similar to a ferromagnetic metal near the unstable point as well as the anomalous behavior of $1/T_1$ in pure $LiV_2O_4$ at low temperatures. The qualitative and quantitative change of $1/T_1$ for Zn substitution will be discussed in the following sections.

## III. ANALYSIS

Here we briefly mention the SCR theory nearby the ferromagnetically unstable point presented by Ishigaki and

Moriya[19] since we mentioned the formula in the previous work,[10] and then we compare with the experimental results for the Zn substituted samples in the present work. $1/T_1$ is proportinal to $\Sigma_q \mathrm{Im}\,\chi(q,\omega_N)/\omega_N$ and is given by using their notation as[19]

$$\frac{1}{T_1}=\frac{3\hbar\gamma_N^2}{4\pi}\frac{A^2}{T_A}\frac{t}{y(t)}, \tag{6}$$

where $A=g\mu_B\ A_{\mathrm{hf}}$, $t=T/T_0$,

$$y=y_0+\frac{3}{2}y_1\int dx x^3\left[\ln u-\frac{1}{2u}-\psi(u)\right], \tag{7}$$

$$u=\frac{x(y+x^2)}{t},\quad \text{and}\quad y_0=\frac{1}{2T_A\chi(T=0)}, \tag{8}$$

respectively. The parameters $y(=1/2T_A\chi)$, $T_0$, and $T_A$ characterize the inverse susceptibility, the energy width, and the distribution of the static susceptibility in $q$ space, respectively. The inverse of the first term in Eq. (7) corresponds to Pauli paramagnetism with Stoner enhancement [see Eq. (15) in the following section]. The value of $y_0$ characterizes a measure of distance from the phase boundary. The second term represents the mode-mode coupling of spin fluctuation. The function $\psi(u)$ in Eq. (7) represents digamma function. Equation (7) is the integral equation with respect to $q$, since $x$ is equal to $q/(6\pi/v_0)^{1/3}$ where $v_0$ represents the volume. The Curie-Weiss-like behavior originates from this term since this term gives rise to $T$-linear dependence in a wide temperature range with the scale of $T_0$. The relaxation rate for $^7$Li is expressed as

$$\frac{1}{T_1}=7.93\times10^2\frac{A_{\mathrm{hf}}^2}{T_A}\frac{t}{y(t)}\quad(\mathrm{sec}^{-1}), \tag{9}$$

where $\gamma_N=16.55$ MHz/KOe is used and the unit of $T_A$ is temperature. The uniform susceptibility with the experimental unit is expressed as

$$\chi=\frac{N(g\mu_B)^2}{2k_BT_Ay(t)}, \tag{10}$$

$$=\frac{1.49}{T_Ay}\quad(\mathrm{emu/mol}) \tag{11}$$

and is related to $1/T_1$ as

$$\frac{1}{T_1}=5.32\times10^2A_{\mathrm{hf}}^2\frac{T\chi}{T_0}. \tag{12}$$

The effect of $y_0$ on $1/T_1$ appears mainly at low temperatures and does not affect at high temperatures. The qualitative behavior of $1/T_1$ depends on the sign of $y_0$. The positive values of $y_0$ correspond to the paramagnetic state, whereas the negative values of $y_0$ correspond to the state with the ordered phase. $1/T_1$ diverges toward the transition temperature for $y_0<0$, whereas $1/T_1$ decreases toward zero with decreasing temperature for $y_0>0$. At phase boundary $y_0=0$, $1/T_1$ diverges as $T^{-1/3}$. The fitting curves together with the experimental data are shown in Figs. 7 and 8. The fitting is possible even for $x=0.4$, however, there remains a question of whether the theory is applicable to the region nearby the MIT point. In the following we show the fitting process or parameters for $x=0$, $x=0.1$, and $x=0.2$ samples.

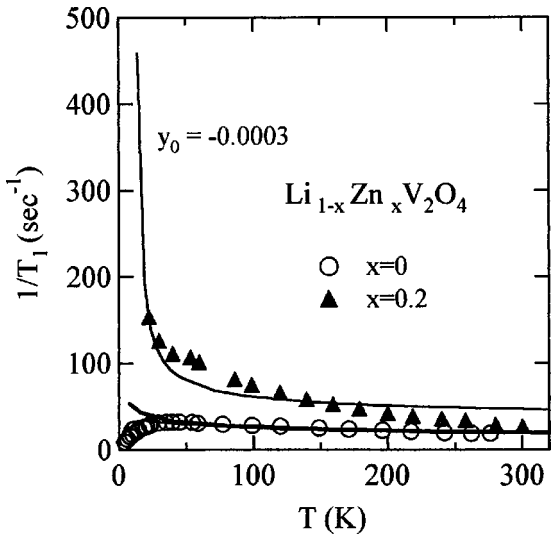


FIG. 8. The fitting of $1/T_1$ on the basis of the SCR theory nearby ferromagnetically unstable point.

### A. $LiV_2O_4$ ($x=0$)

The experimental data were compared with the curves for $y_0=0$ and $6\times10^{-5}$ in the previous work (see Fig. 4 in Ref. 10) by assuming $y_1=0.1$. The same curves are shown in Fig. 7. The curve for $y_0=6\times10^{-5}$ goes down to zero with decreasing temperature, whereas that for $y_0=0$ diverges with decreasing temperature. The same fitting curves for pure $LiV_2O_4$ are also shown in Fig. 8. The value of $T_0$ was chosen as 800 K. We have estimated the value of $T_A$ by assuming $y_1=0.1$ and using the calculated value for $A_{\mathrm{hf}}$ in a previous work. The value of $T_A$ is estimated as 5000 K by using $A_{\mathrm{hf}}=1.71$ KOe/$\mu_B$.

### B. $Li_{1-x}Zn_xV_2O_4$ ($x=0.1$ and 0.2)

The relative values of $T_0$ and $T_A$ compared with pure $LiV_2O_4$ are estimated by considering the Zn concentration dependence of the susceptibility. We denote $T_0$ and $T_A$ for the Zn substituted samples as $T_0(x)=T_0/\alpha$, $T_A(x)=T_A/\beta$, respectively, where $T_0$ and $T_A$ are the values for pure $LiV_2O_4$. Then, the relaxation rate and the susceptibility for the Zn substituted samples, $1/T_1(x)$ and $\chi(x)$, respectively, are expressed as

$$\frac{1}{T_1}(x)=\beta\frac{3\hbar\gamma_N^2}{4\pi}\frac{A^2}{T_A}\frac{\tau}{y(\tau)}\quad\text{and}\quad\chi(x)=\beta\frac{N(g\mu_B)^2}{2k_BT_Ay(\tau)}, \tag{13}$$

where $\tau=\alpha T/T_0$, and they are related with those of the pure one as

$$\frac{1}{T_1(x)T\chi(x)}\Big/\frac{1}{T_1(0)T\chi(0)}=\alpha, \tag{14}$$

where the hyperfine coupling constants for the Zn substituted samples are assumed to be the same as that for the pure one and the contribution of the orbital and diamagnetism is neglected in the susceptibility. According to the SCR theory, $1/T_1$ should be constant at high temperatures. The experimental results of $1/T_1T\chi$ go up with decreasing temperature at low temperatures, since $1/T_1$ increases remarkably with decreasing temperature nearby the transition temperature. However, $1/T_1T\chi$ is likely to approach to constant values at high temperatures, then the relation in Eq. (14) is applicable for high temperatures above 200 K. The values of $\alpha$ are obtained from the data above 200 K as 1.1 and 1.7 for $x=0.1$ and 0.2, respectively. The values of $\beta$ are estimated together with $y_0$ from the fitting of $1/T_1$ as 1.4 and 2.55, whereas $y_0$ is chosen as $-0.0001$ and $-0.0003$, for $x=0.1$ and 0.2, respectively. The fitting curve for the $x=0.2$ sample is shown in Fig. 8. The fact that the value of $\alpha$ increases with increasing Zn concentration implies that the characteristic energy scale of the dynamical susceptibility becomes smaller as Zn concentration increases or the system locates close to the MIT point. The trend seems rather reasonable since the energy range of the dynamical susceptibility for an insulator phase is in general determined by the exchange coupling and is restricted in a smaller region compared to a metal.

## IV. DISCUSSION

We have analyzed the experimental results from the viewpoint of the SCR theory. The main features in the present system are summarized as metal-like conductivity, Curie-Weiss behavior, and $T_1=$const at high temperatures. These features are similar to ferromagnetic metals. Especially, the critical behavior which is expected nearby ferromagnetically unstable point is also seen in the present system. The qualitative difference between pure $LiV_2O_4$ and the Zn substituted samples arises from the sign of $y_0$. The parameter $y_0$ in ferromagnetic metal systems is expressed as

$$y_0 \propto \frac{1-\alpha}{\chi_0(0)} \quad [\alpha = I\chi_0(0)], \tag{15}$$

where $\chi_0(0)$ represents the uniform part ($q=0$) of the susceptibility $\chi_0(q)$ which is determined by the band structure and is obtained from random phase approximation (RPA), whereas $I$ represents the interaction between electrons which includes Coulomb interaction $U$ and exchange interaction $J$. The typical value of the former is usually about 2–3 eV and the latter is 0.5–1 eV in the $d$-electron systems. The uniform susceptibility $\chi_0(0)$ is determined by the density of states $[=2\varrho(\varepsilon_F)]$. The factor $1-\alpha$ corresponds to the Stoner enhancement factor. The ferromagnetic order appears under the condition $1-\alpha<0$. In the present system both cases with the positive and negative signs of $y_0$ are realized by changing Zn concentration. Especially, the reason why pure $LiV_2O_4$ corresponds to the positive sign of $y_0$ is due to the low density of states at Fermi energy as is expected from Eq. (15). The low density of state would be caused by the imperfect screening of the Coulomb interaction. In fact it has been suggested from photoemission experiments[26] that imperfect screening of the Coulomb potential causes low density of states at the Fermi energy in the present system. The reason why the Zn substituted samples correspond to the negative sign of $y_0$ could be attributed to the fact that the interaction $I$ in Eq. (15) becomes larger with increasing Zn concentration. The interaction $I$ is likely to increase with increasing Zn concentration since $ZnV_2O_4$ is a Mott-type insulator. Anyway, the SCR theory is expected to be fundamental to the understanding of anomalous features in $Li_{1-x}Zn_xV_2O_4$ ($0 \leqslant x \leqslant 0.4$).

Although the overall features of this system are qualitatively interpreted from the viewpoint of the SCR theory, there remains some quantitative discrepancies between the susceptibility and $1/T_1$ in pure $LiV_2O_4$. The value of $T_A$ obtained from the susceptibility should be the same as that obtained from $T_1$ if the present system was a perfect ferromagnetic metal. The value estimated from Eq. (12) is 65 000 K. This is one order larger than that obtained from $1/T_1$. As is seen from Eqs. (6) and (10), the ambiguity of $A_{\rm hf}$ may be one of the causes for the discrepancy. However, the discrepancy encountered here is not completely explained by this since $A_{\rm hf}$ should be taken to be about four times larger than the present estimation $A_{\rm hf}=1.71$ KOe/$\mu_B$. The deviation may originate from $q(\neq 0)$ dependence of $\chi(q)$, since $1/T_1$ is affected by all $q$ in $\chi(q)$, whereas only $q=0$ contributes to the uniform susceptibility. The susceptibility $\chi(q)$ may extend to a much wider region in $q$ space compared with usual ferromagnetic metals. However, the orders of $T_A$ and $T_0$ are rather close to those of ferromagnetic metals. In fact the values of $T_0$ have been obtained as 320, 565, 3600 K whereas those of $T_A$ are 12 000, 12 000, and 31 000 K for typical weak ferromagnets $ZrZn_2$, $Sc_3In$, and $Ni_3Al$, respectively.[27] Another difficulty which we have encountered is that the susceptibility calculated by using the parameter $y_0$ obtained from the $1/T_1$ fitting becomes larger than the experimental results at low temperatures below 100 K. This is due to the fact that $y_0$ should be taken as a larger value than that used for $1/T_1$ fitting. In the case where $y_0$ is treated as a constant, $I$ in Eq. (15) is regarded as a short range interaction of $\delta$-function type in the real space originating from the screening effect of the Coulomb interaction. The effects of $q$ dependence or imperfect screening in the exchange interaction and Coulomb interaction, or the effect of a random potential due to Zn substitution could be important to explain the difficulty. These factors are also related to the first discrepancy since these factors would affect the band structure, the density of states at Fermi energy, and $\chi_0(q)$. Further theoretical investigation is needed for the precise understanding of this system.

We have suggested the importance of $q=0$ component in $\chi(q)$ to understand the nature of this system for the metal-like region. The $q=0$ component is also important for the region $0.4 \leqslant x \leqslant 1$, since the $T$ and Zn concentration dependences of $1/T_1$ also correspond to those of the susceptibility. The value of the susceptibility increases with decreasing temperature toward the transition temperature in a way similar to the metal-like region, however the values at fixed temperatures become smaller as Zn concentration increases in this region. The value of the susceptibility takes the maximum at $x=0.4$–$0.5$ in the overall range of $x$ at fixed temperatures above 100 K as mentioned in the Introduction. $1/T_1$

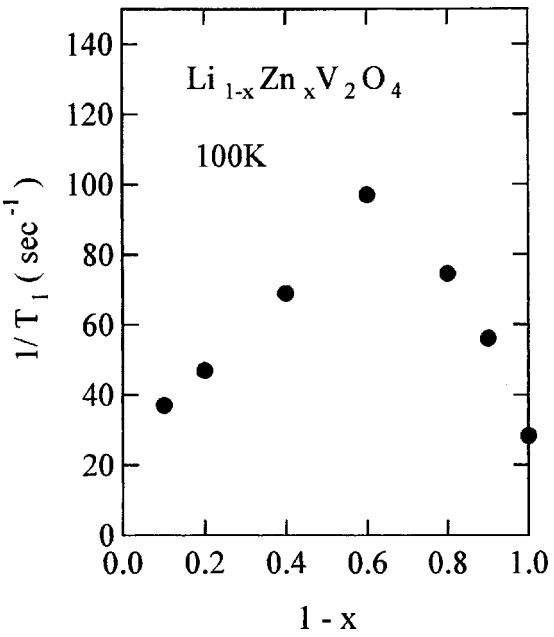


FIG. 9. Zn concentration dependence of $1/T_1$ at 100 K.

also shows the same behavior, that is, the maximum of $1/T_1$ appears at $x=0.4$–$0.5$ at fixed temperatures as shown in Fig. 9. The analysis presented in the previous section is not applied for $0.4 \leqslant x \leqslant 1$ and other relaxation mechanisms for a semiconductor or an insulator are required.

## V. CONCLUSION

We have performed nuclear magnetic resonance for $^7$Li nuclei in vanadium spinel $Li_{1-x}Zn_xV_2O_4$ ($0 \leqslant x \leqslant 0.4$) from 4.2 to 300 K. We found that the relaxation rate $1/T_1$ and the linewidth for $x \neq 0$ samples qualitatively differ from those for the pure $LiV_2O_4$. $1/T_1$ and the linewidth for $x \neq 0$ samples show a monotonous increase with decreasing temperature toward the order point appearing at about 15 K, whereas for pure $LiV_2O_4$, a paramagnetic metal, $1/T_1$ and the linewidth remain finite values although both show anomalies at 50 and 20 K, respectively. These anomalous features in $1/T_1$ appearing by Zn substitution is also seen in the susceptibility, which implies that the $q=0$ mode plays an important role to understand the overall nature of this system. On the basis of these experimental facts, $1/T_1$ and the susceptibility were investigated from the viewpoint analogous to ferromagnetic metal systems. The overall features including anomalous behavior in $Li_{1-x}Zn_xV_2O_4$ ($0 \leqslant x \leqslant 0.4$) were qualitatively interpreted as the critical phenomena nearby the ferromagnetically unstable point, although some modification is necessary for the quantitatively precise agreement with the real materials.

## ACKNOWLEDGMENT

We would like to thank T. Urano, Professor H. Takagi, and Dr. S. Kondo of ISSP, University of Tokyo for private communication.

[1] D. B. Rogers, J. L. Gilson, and T. E. Gier, Solid State Commun. **5**, 263 (1967).
[2] K. Kawakami, Y. Sakai, and N. Tsuda, J. Phys. Soc. Jpn. **55**, 3174 (1986).
[3] B. Reuter and K. Muller, Naturwissenschaften **54**, 164 (1967).
[4] Y. Ueda, N. Fujiwara, and H. Yasuoka, J. Phys. Soc. Jpn. **66**, 778 (1997).
[5] Muhtar , F. Takagi, K. Kawakami, and N. Tsuda, J. Phys. Soc. Jpn. **7**, 119 (1998).
[6] S. Niziol, Phys. Status Solidi A **18**, K11 (1973).
[7] T. Urano and H. Takagi (private communication).
[8] S. Kondo *et al.*, Phys. Rev. Lett. **78**, 3729 (1997).
[9] N. Fujiwara, H. Yasuoka, and Y. Ueda, Physica B **59-60**, 237 (1997).
[10] N. Fujiwara, H. Yasuoka, and Y. Ueda, Phys. Rev. B **57**, 3539 (1998).
[11] A. V. Mahajan, R. Sala, E. Lee, F. Borsa, S. Kondo, and D. C. Johnston, Phys. Rev. B **57**, 8890 (1998).
[12] K. Kadowaki and S. B. Woods, Solid State Commun. **58**, 507 (1986).
[13] S. Kondo, D. C. Johnston, and L. L. Miller, Phys. Rev. B **59**, 2609 (1999);D. C. Johnston, C. A. Swenson, and S. Kondo, *ibid.* **59**, 2627 (1999).
[14] H. Yasuoka, V. Jaccarino, R. C. Sherwood, and J. H. Wernick, J. Phys. Soc. Jpn. **44**, 842 (1978).
[15] M. Kontani, T. Hioki, and Y. Masuda, J. Phys. Soc. Jpn. **39**, 665 (1975).
[16] T. Hioki and Y. Masuda, J. Phys. Soc. Jpn. **43**, 1200 (1977).
[17] H. Saji, T. Yamadaya, and M. Asanuma, J. Phys. Soc. Jpn. **21**, 255 (1966).
[18] K. Ueda and T. Moriya, J. Phys. Soc. Jpn. **38**, 32 (1975).
[19] A. Ishigaki and T. Moriya, J. Phys. Soc. Jpn. **65**, 3402 (1996).
[20] A. Ishigaki and T. Moriya, J. Phys. Soc. Jpn. **65**, 376 (1996).
[21] P. W. Selwood, *Magnetochemistry*, 2nd ed. (Interscience, New York, 1956).
[22] A. H. Morrish, *The Physical Principles of Magnetism* (Wiley, New York, 1965).
[23] Y. Amako, T. Naka, M. Onoda, H. Nagasawa, and T. Erata, J. Phys. Soc. Jpn. **59**, 2241 (1996).
[24] M. Onoda, H. Imai, Y. Amako, and H. Nagasawa, Phys. Rev. B **56**, 3760 (1997).
[25] W. M. Lomer, Proc. Phys. Soc. London **80**, 1380 (1962).
[26] A. Fujimori, K. Kawakami, and N. Tsuda, Phys. Rev. B **38**, 7889 (1998).
[27] T. Moriya, in *Spin Fluctuations in Itinerant Electron Magnetism*, Vol. 56 of *Springer Series in Solid-State Science* (Springer, Berlin, 1985).